

An effective nanostructured green phosphor $\text{Zn}_2\text{SiO}_4:\text{Mn}^{2+}$ prepared by sol-gel method

K. A. Sergeeva¹, A. A. Sergeev², A. A. Rempel^{1,3}

¹Ural Federal University, Mira, 19, Ekaterinburg, 620002, Russia

²Far-Eastern Federal University, Sukhanova, 8, Vladivostok, 690091, Russia

³Institute of Metallurgy, Ural Branch of the Russian Academy of Sciences, Amundsena, 101, Ekaterinburg, 620016, Russia

kspetrovyh@mail.ru

PACS 78.55.-m, 81.20-n

DOI 10.17586/2220-8054-2018-9-4-507-512

A nanostructured willemite doped with manganese ($\text{Zn}_2\text{SiO}_4:\text{Mn}^{2+}$) was synthesized by sol-gel method followed by high-temperature annealing. Prepared $\text{Zn}_2\text{SiO}_4:\text{Mn}^{2+}$ is characterized by average particle size of 100 nm, narrow particle size distribution, and high crystallinity. Under UV-excitation nanostructured willemite shows an intensive photoluminescence at 520 nm corresponded to activator Mn^{2+} emission. It was found that the emission decay curves of willemite becomes non-exponential with increasing of manganese content. $\text{Zn}_2\text{SiO}_4:\text{Mn}^{2+}$ reveals long-lasting phosphorescence up to 45 ms. Absolute quantum yield of $\text{Zn}_2\text{SiO}_4:\text{Mn}^{2+}$ reaches 47 % at 0.1 at. % of Mn^{2+} . The luminescence concentration quenching effect at Mn^{2+} concentration higher than 1 at % is observed.

Keywords: willemite, manganese, photoluminescence, quantum yield.

Received: 10 July 2018

1. Introduction

Wide band gap semiconductor oxide phosphors doped with ions of transition and/or rare-earth metals are used extensively to create optical and luminescent instruments for various purposes. At the same time, the field of application is not limited to bulk microcrystalline materials, but includes nanostructured powders, thin films and multilayer coatings consisting of nanoparticles from 1 to 100 nm. The main benefits of nanostructured phosphors are increase of luminescence brightness, higher adhesion to the substrate, large specific surface, etc. [1].

Willemite, activated by manganese, or $\text{Zn}_2\text{SiO}_4:\text{Mn}^{2+}$, is one of the brightest representatives of oxide phosphors. Manganese ions, embedded in the crystal lattice of zinc orthosilicate, form a solid substitutional solution, which leads to a change in the optical and photoluminescent (PL) properties of the material [2]. Since the band gap of willemite is 5.0 – 6.2 eV, under UV-excitation (3 – 5 eV) the intracenter absorption and emission of photons within the $3d^5$ electron shell of Mn^{2+} ions is the dominant process [3]. To date, the mechanisms of energy transfer in $\text{Zn}_2\text{SiO}_4:\text{Mn}^{2+}$ under interband excitation, as well as competition between the interband and intracenter relaxation, the nature of the intrinsic defects of the matrix and their interaction with activator ions remain insufficiently studied. The effect of the nanostructured state and the activator concentration on the spectral and kinetic characteristics of the willemite is of great importance for practical applications.

The aim of this work was the analysis of the spectral and kinetic parameters of photoluminescence of nanostructured $\text{Zn}_2\text{SiO}_4:\text{Mn}^{2+}$, prepared by sol-gel method, depending on the crystallinity degree of the structure, the particle size and the concentration of the Mn^{2+} activator.

2. Experimental

2.1. Synthesis

Nanostructured $\alpha\text{-Zn}_2\text{SiO}_4:\text{Mn}^{2+}$ was prepared by sol-gel method followed by high-temperature annealing. Zinc nitride $\text{Zn}(\text{NO}_3)_2$, manganese acetate $\text{Mn}(\text{CH}_3\text{COO})_2$, and tetraethylorthosilicate (TEOS) $\text{Si}(\text{OC}_2\text{H}_5)_4$ were used as sources of zinc, manganese and silicon, respectively. The stoichiometric ratio of mixture components was $\text{Zn}_{2-x}\text{SiO}_4:\text{Mn}_x$, where x varies from 0 to 0.35. Appropriate amounts of metal salts were diluted in ethanol, and then TEOS was added. The mixture was stirred for 3 h. The pH of the mixture was adjusted to approximately 2 by dropwise addition of HNO_3 . To initiate hydrolysis, water was added in the volume ratio of $V_{\text{EtOH}}:V_{\text{H}_2\text{O}} = 10:1$. Prepared sol was transparent and sediment-free. The gelation process was initiated by subjecting of sols in boiled water bath within 1 h. After that, the gels were dried in a drying oven at 300 °C for 5 h. To form the $\alpha\text{-Zn}_2\text{SiO}_4$ crystalline modification the dried powders were annealed in air at temperatures ranging from 500 – 1000 °C for 5 h.

2.2. Characterization

The crystal structure and phase composition of prepared $\text{Zn}_2\text{SiO}_4:\text{Mn}^{2+}$ was investigated by X-ray diffraction (Shimadzu XRD MAXIMA) in the Bragg-Brentano geometry. The crystallinity degree was determined as the ratio of $\alpha\text{-Zn}_2\text{SiO}_4$ diffraction peak intensity to intensity of diffusive halo in the willemite diffraction pattern. The average particle size in $\text{Zn}_2\text{SiO}_4:\text{Mn}^{2+}$ was calculated by Williamson–Hall method [4] as:

$$\langle D_{CSR} \rangle = 1/\beta^*(2\theta = 0), \quad (1)$$

where $\beta^* = \cos \theta \cdot \beta(2\theta)$ is normalized diffraction peak broadening, $1/\text{nm}^{-1}$; 2θ is X-Ray scattering angle.

The particle size distribution in nanostructured $\text{Zn}_2\text{SiO}_4:\text{Mn}^{2+}$ was investigated by dynamic light scattering (Malvern Zetasizer Nano ZS). The 633 nm laser light scattering angle was 13° . The nanopowders were preliminary dispersed in ethanol-water solution and stirred by SONOPULS ultrasonic homogenizator (Bandelin).

The diffuse reflection spectra of $\text{Zn}_2\text{SiO}_4:\text{Mn}^{2+}$ nanopowders in the range from 220 to 800 nm was recorded by Cary Varian 5000 spectrometer using an integrated sphere. The optical band gap was determined by Tauc method [5]:

$$(h\nu F(r))^{\frac{1}{n}} = A(h\nu - E_g), \quad (2)$$

where E_g is fundamental band gap, eV; h is Plank constant, J·s; ν is electromagnetic wave oscillation frequency, Hz; $F(r) = (1 - r_\infty)^2/2r_\infty$ is Kubelka–Munc function; A is a constant. For the willemite exponent, n is equal to $1/2$ corresponding to direct transition.

The photoluminescence emission and excitation (PLE) spectra of nanostructured willemite were recorded using Horiba Fluorolog 3 spectrometer. PLE spectra was normalized to xenon lamp emission specter. PL decay measurements were performed in the range of 0 to 150 ms and initial delay of 0.05 ms with the same equipment.

The PL decay curves were fitted using superposition of stretched and simple exponential functions:

$$I(t) = I_1 \exp \left[- \left(\frac{t}{t_1} \right)^\beta \right] + I_2 \exp \left[- \frac{t}{t_2} \right], \quad (3)$$

where β is the degree of nonexponentiality.

The absolute quantum yield (AQY) was calculated as the ratio of emitted photons to absorbed ones:

$$\varphi_{abc} = \frac{E_c - E_a}{L_a - L_c}, \quad (4)$$

where E_c is integrated PL intensity of the sample; E_a is integrated PL intensity of the integrated sphere; L_c is integrated PLE intensity of the sample; L_a is integrated PLE intensity of the integrated sphere.

3. Results and discussion

Figure 1 shows the XRD patterns of $\text{Zn}_2\text{SiO}_4:\text{Mn}^{2+}$ in dependence on the annealing temperature and manganese content. After annealing at 1000°C , all the samples are characterized with 100 % of $\alpha\text{-Zn}_2\text{SiO}_4$ crystal phase (Fig. 1a). One should note that the crystallinity of obtained willemite is higher than in case of ZnCl_2 precursor used in previous study [6]. The amount of manganese (in the chosen range from 0.1 to 5 at.%) does not affect the crystallinity degree of $\alpha\text{-Zn}_2\text{SiO}_4:\text{Mn}^{2+}$ (Fig. 1b). The absence of other willemite modifications and manganese-related crystal phases indicates the formation of homogeneity activator-matrix solid solution. The average particle size of $\text{Zn}_2\text{SiO}_4:\text{Mn}^{2+}$ rises from 60 to 100 nm with Mn^{2+} content increasing.

Fig. 2 shows the particle size distribution of nanostructured willemite in ethanol-water solution. It was found that the distribution function is bimodal and indicates the particles of 130 nm and about 700 nm. The smaller particle size is in good correlation with the XRD data. The fact that the particles of 700 nm are observed can be explained as both nonsolubility of $\text{Zn}_2\text{SiO}_4:\text{Mn}^{2+}$ and a tendency of smaller particles to agglomerate. The particle size distribution function is independent of manganese concentration.

The diffusive reflection and PLE spectra of nanostructured willemite are shown in Fig. 3. Independent of manganese content, there is an absorption in the region of 5 eV and higher. That corresponded to fundamental absorption edge of Zn_2SiO_4 , which is close to 5.8 eV according to different estimates [7, 8]. Willemite doped with Mn^{2+} are characterized by an additional absorption edge at 3.5 eV. That value is well-correlated with PLE bands in the same region related to excitation within $3d^5$ electron shell of Mn^{2+} . One can add that the absorption in 3.5 eV is observed also for undoped willemite. That is possible due to uncontrollable manganese impurity in precursors (<0.005 at.%). The optical band gap estimated by Tauc method varies from 5.6 to 4.0 eV for undoped willemite and the sample with 5 at.% of Mn^{2+} , respectively.

It was found that even low-crystalline willemite (30 % – 600°C) under excitation at 5.0 eV exhibits a broad PL band with maximum at 515 nm (Fig. 4). The PL maximum and structure correspond to ${}^4T_1 \rightarrow {}^6A_1$ transition

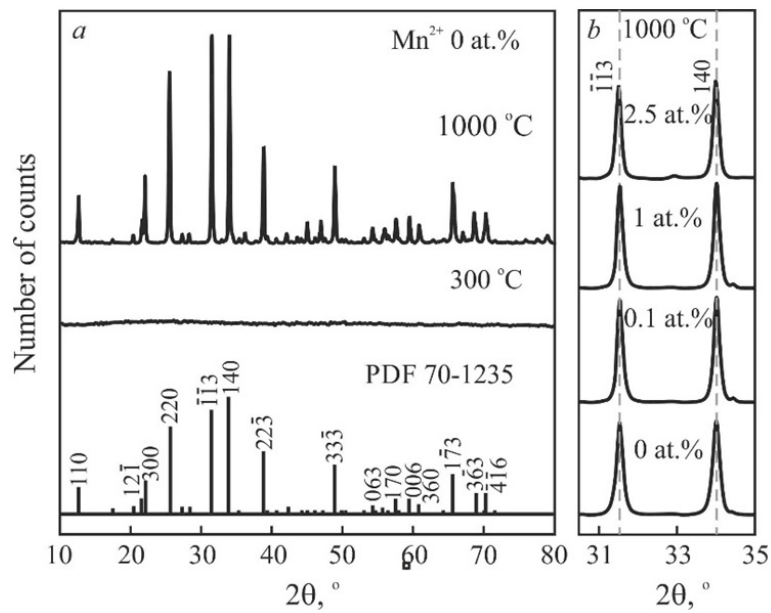


FIG. 1. X-ray diffraction patterns of nanostructured $\text{Zn}_2\text{SiO}_4:\text{Mn}^{2+}$ depending on the annealing temperature (a) and manganese content (b)

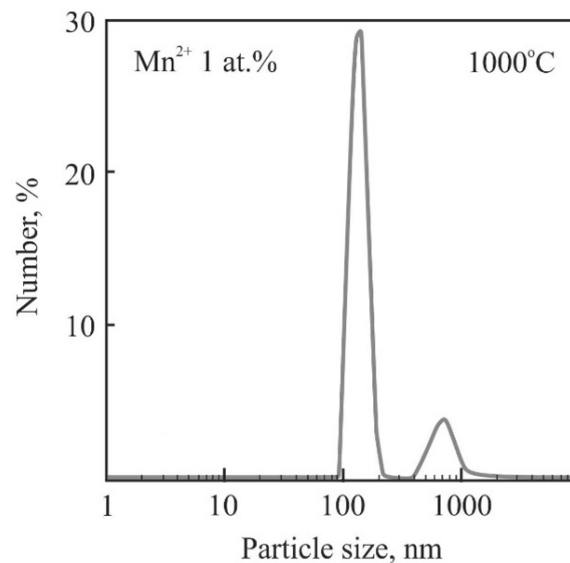


FIG. 2. Particle size distribution in willemite dispersed in ethanol-water solution

within $3d^5$ electron shell of Mn^{2+} . Increasing the annealing temperature to 1000 °C leads to PL band rising while its maximum shifts to 525 nm. The observed PL intensity rising is due to crystallinity improvement, residual OH group elimination, and increasing of the nanoparticle surface roughness [9].

The PL decay curves of $\text{Zn}_2\text{SiO}_4:\text{Mn}^{2+}$ at low manganese concentrations (<0.1 at. %) has an exponential form since all the activator ions are single (has no nearest neighbors of the same type) (Fig. 5a). As Mn^{2+} content is increased, the decay becomes stretched exponential due to the presence of different types of luminescence centers (Mn^{2+} pairs and next nearest neighbors) and energy transfer from isolated Mn^{2+} ions to the pairs. All the centers could be excited both directly and by nonradiative energy transfer that causes the range of charge carrier recombination time [10]. The non-exponentiality degree β varies from 0.55 to 0.9. Long-lasting phosphorescence of the nanostructured willemite (average decay time $\tau_{1/e}$ is up to 45 ms) is caused by the release of the electrons from deep traps. The PL rising stage for 2 ms also indicates the process of interaction between the traps and activator ions. It was supposed that the oxygen vacancies may act as the traps in Zn_2SiO_4 crystal lattice [11].

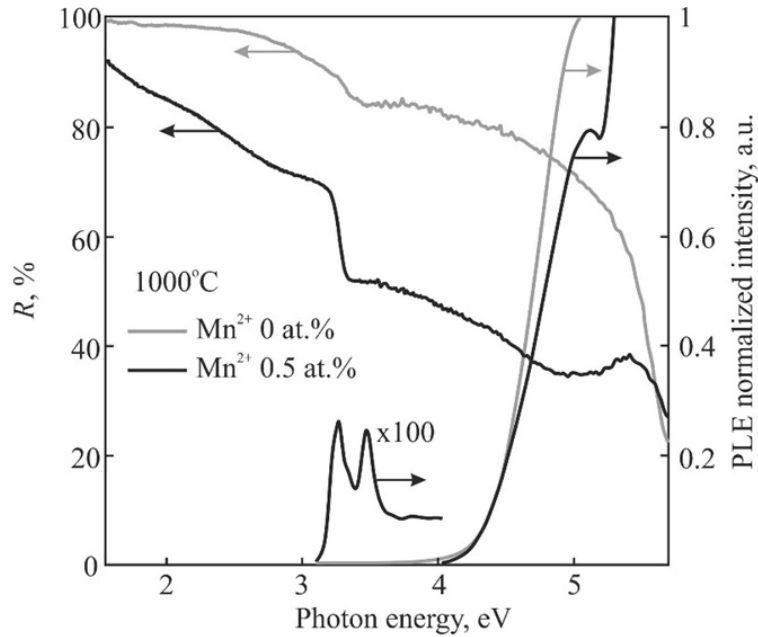


FIG. 3. The diffusive reflection and PLE spectra of nanostructured $\text{Zn}_2\text{SiO}_4:\text{Mn}^{2+}$ in dependence of manganese concentration

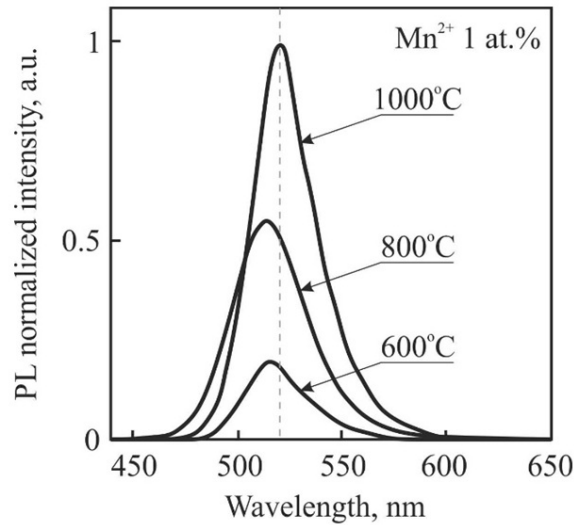


FIG. 4. PL spectra of nanostructured $\text{Zn}_2\text{SiO}_4:\text{Mn}^{2+}$ (1 at. %) depending on the annealing temperature

The threshold concentration of manganese in the obtained nanostructured $\text{Zn}_2\text{SiO}_4:\text{Mn}^{2+}$ is found to be equal to 1 at. % (Fig. 5b). After reaching the threshold concentration, the possibility of radiation-free energy transfer between nearest Mn^{2+} ions becomes higher than the possibility of radiative recombination in single Mn^{2+} . That leads to the significant PL quenching at high manganese content. As a result of exchange coupling between Mn^{2+} pairs, the average decay time is shortening from 45 to 1 ms (5 at. % Mn^{2+}).

Sol-gel, prepared $\text{Zn}_2\text{SiO}_4:\text{Mn}^{2+}$ nanopowder and nanostructured willemite ceramics, obtained earlier by solid state sintering of nanopowders [12], show almost four times higher PL efficiency comparing with commercial microcrystalline powder (Fig. 6). It is caused by large specific surface of nanostructured phosphor that provides significant adoption of activator ions. In addition, sol-gel method provides willemite with high crystallinity, homogeneity, and better manganese incorporation in Zn_2SiO_4 crystal lattice than conventional solid-state reaction. Along with high AQY nanostructured willemite is characterized by PL decay time in wide range of 6 – 45 ms.

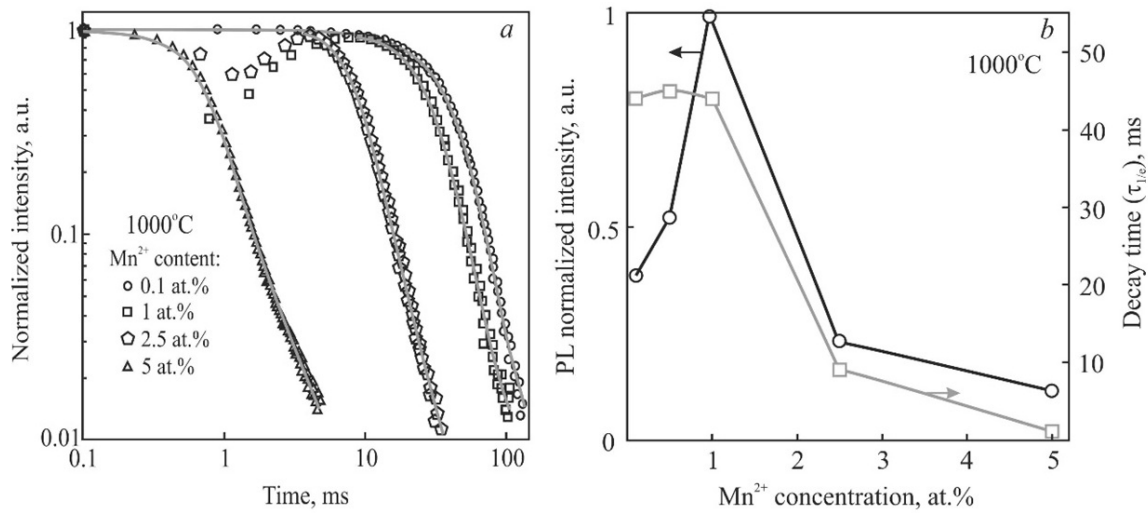


FIG. 5. PL decay curves (a); PL intensity and average decay time (b) depending on manganese content in $Zn_2SiO_4:Mn^{2+}$

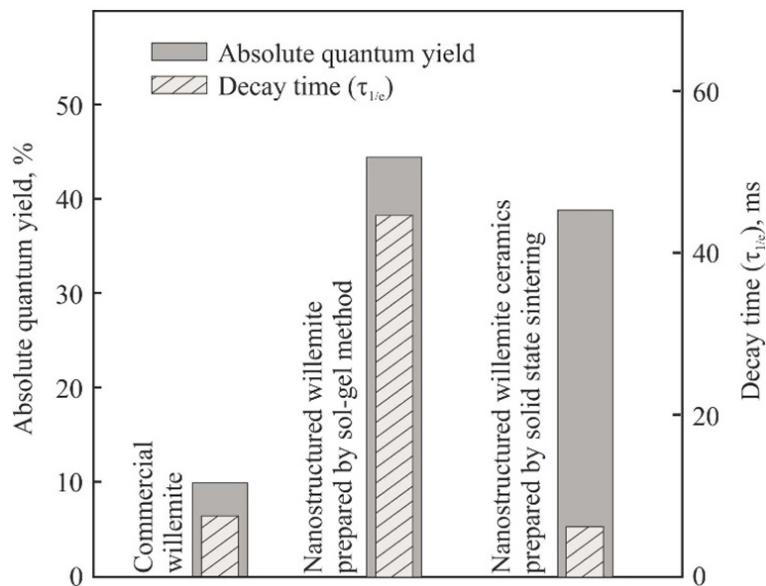


FIG. 6. Absolute quantum yield and PL decay time of microcrystalline willemite (FGI-520), $Zn_2SiO_4:Mn^{2+}$ nanopowders obtained by sol-gel method and nanostructured willemite ceramics

4. Conclusions

Nanostructured monodispersed $Zn_2SiO_4:Mn^{2+}$ with a particle size of 100 nm, high crystallinity and homogeneity was prepared by sol-gel method. The structure and maximum position of PL spectra confirmed the formation of $Mn-Zn_2SiO_4$ solid solution. The absolute quantum yield of luminescence of the obtained willemite is four times higher than of commercial one. Long decay time (45 ms) makes it possible to use $Zn_2SiO_4:Mn^{2+}$ as a phosphor in medical and radar devices. While the nanostructured willemite ceramics characterized by high efficiency and rather short decay time of 6 ms is promising material for plasma display panels and optical devices in which short response time is required.

Acknowledgement

This work was supported by Act 211 Government of the Russian Federation, contract No 02.A03.21.0006. The authors are grateful to Minobrnauki initiative project No 16.5186.2017/8.9.

References

- [1] Suzdalev I.P. *Nanotechnology: Physics and Chemistry of nanoclusters, nanostructures and nanomaterials*. Kom.Kniga, Moscow, 2006, 592 p.
- [2] Stevels A.L.N. Recent developments in the application of phosphors. *Journal of Luminescence*, 1976, **12**, P. 97–107.
- [3] Ilmas E.R., Savikhina T.I. Investigation of luminescence excitation processes in some oxygen-dominated compounds by 3 to 21 eV photons. *Journal of Luminescence*, 1970, **1**, P. 702–715.
- [4] Williamson G.K., Hall W.H. X-ray line broadening from field Aluminium and Wolfram. *Acta Metallurgica*, 1953, **1**, P. 22–31.
- [5] Kortyum G., Braun V., Gertsog G. Principles and methods of registration in diffusive reflectance spectroscopy. *Physics-Uspokhi (Advances in Physical Sciences)*, 1965, **85**(2), P. 365–380.
- [6] Petrovykh K.A., Rempel A.A., Kortov V.S., Buntov E.A. Sol-gel synthesis and Photoluminescence of nanosized $\text{Zn}_2\text{SiO}_4\text{:Mn}$. *Inorganic materials*, 2015, **51**(2), P. 152–157.
- [7] Karazhanov S.Z., Ravindran P., Fjellvåg H., Svensson B.G. Electronic structure and optical properties of ZnSiO_3 and Zn_2SiO_4 . *Journal of Applied Physics*, 2009, **106**, P. 123701.
- [8] El Ghoul J., El Mir L. Sol-gel synthesis and luminescence of undoped and Mn-doped zinc orthosilicate phosphor nanocomposites. *Journal of Luminescence*, 2014, **148**, P. 82–88.
- [9] Tsai M.T., Lin Y.H., Yang J.R. Characterization of Manganese-doped Willemite Green Phosphor Gel Powders. *IOP Conference Series: Materials Science and Engineering*, 2011, **18**, P. 32026.
- [10] Vink A.P., de Bruin M.A., Roke S., Peijzel P.S., Meijerink A. Luminescence of Exchange Coupled Pairs of Transition Metal Ions. *Journal of The Electrochemical Society*, 2001, **148**, P. E313–E320.
- [11] Dubey V., Tiwari R., Pradhan M., Rathore G., Sharma C., Tamrakar R. Photoluminescence and Thermoluminescence Behavior of $\text{Zn}_2\text{SiO}_4\text{:Mn}^{2+}$, Eu^{2+} Phosphor. *Journal of Luminescence and Applications*, 2014, **1**, P. 30–39.
- [12] Kortov V.S., Sergeeva K.A., Pustovarov V.A., Rempel A.A. Photoluminescence of nanosized $\text{Zn}_2\text{SiO}_4\text{:Mn}^{2+}$ ceramics under UV- and VUV-excitation. *Journal of Surface Investigation: X-Ray, Synchrotron and Neutron techniques*, 2017, **7**, P. 49–54.